water

MDPI

Article

Karst Recharge Areas Identified by Combined Application of Isotopes and Hydrogeological Budget

Silvia Iacurto, Gerardo Grelle, Francesco Maria De Filippi and Giuseppe Sappa *

Department of Civil, Constructional and Environmental Engineering (DICEA), Sapienza University of Rome, 00184 Rome, Italy; silvia.iacurto@uniroma1.it (S.I.); gerardo.grelle@uniroma1.it (G.G.); francescomaria.defilippi@uniroma1.it (F.M.D.F.)

* Correspondence: giuseppe.sappa@uniroma1.it; Tel.: +39-0644-585-010 or +39-3452-808-882

Abstract: The identification of recharge areas in karst aquifers allows us to perform sustainable management of these groundwater resources. Stable isotopes ($\delta^{18}O$ and $\delta^{2}H$) have been largely used to provide information about recharge elevation in many mountainous regions. In this paper, an improved version of a recent "isotope-driven model", for the identification of recharge areas, was applied to Capodacqua di Spigno Spring (south of the Latium region). The model upgrade consists of a preliminary check procedure to estimate the degree of influence of the rainfall's isotopic variability on the spring water. This additional procedure gives us an indication of the reliability of the model and its applicability conditions. Moreover, the dataset of the spring was updated to analyze the degree of reliability of the isotope-driven model. The purpose of this study was to combine the previously mentioned isotope-driven model with hydrogeological tools. A quantitative study of the basin, based on the estimation of the average monthly infiltration volume, was performed by using the inverse hydrogeological water budget. In this way, the qualitative model for the recharge areas' estimation was validated by a quantitative hydrogeological tool. Both models show that, for karst mountain basins, the recharge areas decrease as the average recharge elevations increase, including areas at high altitudes.

Keywords: recharge area; karst aquifer; stable isotope; inverse hydrogeological water budget; isotopic tracers; spring discharge; rainfall isotopic variability

Citation: Iacurto, S.; Grelle, G.; De Filippi, F.; Sappa, G. Karst Recharge Areas Identified by Combined Application of Isotopes and Hydrogeological Budget. *Water* **2021**, *13*, 1965. https://doi.org/10.3390/w13141965

Received: 19 May 2021
Accepted: 13 July 2021
Published: 17 July 2021

1. Introduction

Karst groundwater is a primary source of freshwater in many regions around the world. About 25% of the global population is partly or entirely supplied by freshwater from karst. Most of the largest springs in the world are located in karst areas [1]. It was estimated that the percentage of karst water consumers in 2016 was 9.2% of the world's population [2]. Indeed, for a large part of the Mediterranean region, karst springs play an essential role for water supply. Karst springs provide fresh and high-quality water, which has been an important resource for human development in this region since antiquity [3]. Specifically, in Italy, the karst carbonate aquifers of the central Apennines represent the largest groundwater reservoir [3,4].

Therefore, for the protection and sustainable management of groundwater resources, it is critical to study the recharge–discharge mechanism of a karst aquifer and determine the recharge areas [5]. These aquifers are very complex systems, as each one has its own distinctive characteristics [6,7]. The high spatial heterogeneity of a karst aquifer, often characterized by poor available data, requires specific investigation techniques such as environmental tracers. At the common temperature of groundwater, there is no sensitive isotope exchange between the groundwater and minerals. Therefore, stable isotopes such as ^{2}H and ^{18}O can act as conservative tracers [8]. In this framework, the isotopic tracers play a key role. As the basic conceptual model, it is possible to claim that the isotopic

composition and concentration values are affected by a number of environmental variables, which affect evapotranspiration output. Starting from Dansgaard (1964) [9], many attempts were undertaken to include the relationship of the isotopic composition of monthly precipitation with the latitude, altitude and amount of precipitation, the distance from the coastline, and the air temperature [10]. Some of these effects have local variability and were represented by the Local Meteoric Water Line (LMWL) [11,12]; in this way, light changing of the ^{2}H to ^{18}O ratio also identifies a specific composition marker for an assigned meteorological region. In addition to this regional behavior, other local effects contribute to change in the rainfall's isotopic concentration. Among these ones, the altitude–topographic effect seems to have a relevant role in mountainous areas. This effect is related to the evapotranspiration of air that induces an enrichment of the heavy-isotopic content during precipitation, up to the time the rainwater reaches the soil surface. The enrichment is strictly due to the air temperature gradient and the travel time from the clouds to the topographic surface. Therefore, in mountainous environments, the isotopic concentration of the rainwater impacting the soil is strictly linked to the altitude at which it happens [12]. Stable isotopes may be used as conservative tracers to understand water dynamics, e.g., groundwater recharge areas, its source and movement [13,14]. Water isotopes are a natural part of the water molecule, and so these can be regarded as the most ideal tracer. Combined studies on natural tracers, such as isotopes, and spring discharge may provide integrated knowledge regarding the key characteristics of the karst groundwater system [15]. Oxygen-18 and deuterium have been largely used to determine groundwater recharge areas, with their elevations, transit times and water flow paths [16–20]. Considering the local vertical isotopic gradient, the isotopic values of groundwater can be used to identify the average recharge area elevation of aquifers [17]. This average elevation can be estimated starting from the $\delta^{18}O$ and $\delta^{2}H$ values of the water sampled, at a known altitude, in a pluviometric station located near the study area. Identifying a specific elevation at which groundwater has infiltrated is a technique frequently applied in isotope hydrology [10,17]. This, however, assumes that the spring sample is the product of rainwater infiltration at a single elevation, which is a strong simplification. In fact, the elevation identified by the isotope is always an average recharge elevation. Based on this consideration, an isotope-driven model has been set up [21], which estimates, for any discharge value of a spring, the percentage of the topographic area involved in the aquifer recharge and its spatial distribution. Specifically, the model identifies the main recharge areas according to the oxygen and hydrogen isotopes' ($\delta^{18}O$ and $\delta^{2}H$) rates of variation, which are detected in groundwater samples taken at the spring. Considering this framework, the identification of recharge areas has a relevant role for a proper water governance, with the aim of safeguarding spring water quality.

Objectives

The present study focuses on the identification of recharge areas for karst springs by the combined application of stable isotopes ($\delta^{18}O$ and $\delta^{2}H$) and hydrogeological budget. The latter is performed using the empirical method for estimating potential evapotranspiration (PET) proposed by Thornthwaite (1948) [22], applied to the inverse hydrogeological budget method (IHBM) [23–25]. Specifically, in the present study, the previously mentioned isotope-driven model [21] has been improved. The model extension consists of a preliminary check procedure to estimate the influence degree of seasonality combined with amount effect of rainfall (input) on spring water (output). This additional procedure aims to give an overview of the favorable conditions to the applicability of the model. Moreover, in this study, the updating of the previous dataset, regarding Capodacqua di Spigno Spring (in the southern part of the Latium region), made it possible to verify the consistency and soundness of the model.

2. Study Area Characterization

2.1. Geological and Hydrogeological Setting of the Study Area

Capodacqua di Spigno Spring, one of the main groundwater outlets in the southeast Latium region, is sited in the province of Latina, about 4 km from the Tyrrhenian Sea [21]. This spring, located at the bottom of Petrella Mountain, has been known since Roman times. In 72 BC, the emperor Vespasian built an 11 km long aqueduct that collected spring waters to supply the city of Minturno (LT). The current aqueduct of Capodacqua di Spigno Spring feeds the larger area including Spigno Saturnia, Formia and Esperia municipalities, in Latina province [26] (Figure 1). The aquifer's altitude ranges from about 100 m a.s.l. to about 1500 m a.s.l., with an average value of 880 m a.s.l; the limits of the aquifer are assumed considering the watershed topographic pattern. The altitude of the spring, instead, is of 35 m a.s.l. This spring is located in the karst coastal region of the western Aurunci Mountains, which, together with the Lepini and the Ausoni Mountains, belong to the Pre-Apennines of Latium and form the carbonatic platform of the Volsci Ridge, separated from the Apennine ridge by the Latina Valley [21]. The spring water comes out from the permeable limestone of La Civita Mountain and Castello Mountain and flows above the Upper Miocene clays, at the lowest point of the limestone–clay contact [27]. The water table map described by previous studies [28] shows that the main direction of the aquifer is generally south–south east. Differently, there are also important local flows along the two faults, which delimit the carbonate series outcropping, especially the one to the east, which seems to represent the main water conduit towards the spring. More detailed geological information on the study area can be derived from previous studies [28]. The stratigraphic succession of the soils, from the bottom upwards, is as follows:.

- Carbonate Series (CS1): limestone-–dolomite series that forms the western Aurunci Mountains (stratigraphic alternation Palaeocene–Upper Lias; sedimentary marine facies);
- Kaolinitic Clays (KC): consisting of a polychrome clay–silty blanket (marginal marine siltstone facies);
- Clutch Breach (Br);
- Miocene Series (MS): formed by the grouping of two hydrogeologically similar formations (marine to continental–marine transitional facies);
- Deposits of the lower Pliocene (p) (continental–marine facies);
- Quaternary deposits (q): river and lake deposits and groundwater debris (continental facies).

The Carbonate Series (CS1), present in the area of the Capodacqua di Spigno basin, is characterized by limestones and dolomites (Palaeocene—Upper Lias) alternations. As found in the Geological Map of Italy (scale 1:100,000, sheet no. 171 "Gaeta") [29] referring to the area under study, identified by the Civita Mountain, the aforementioned Carbonate Series (CS1) is divided into two formations: a younger Carbonate Series formed in the Cretaceous period and an older one formed during the Jurassic period. Therefore, in the geological stratigraphic succession, the Carbonate Series (CS1), Jurassic carbonate Series (JCS) and Cretaceous Carbonate Series (CCS) were taken into consideration. Figure 1 depicts a sketch of the structural setting of the Volsci chain. This scheme has been modified starting from that proposed by Baldi et al. in 2005 [28]. The new interpretation of the geology and structural characteristics of the area came from the study of both the Geological Map of Italy (scale 1:100,000, sheet no. 171 "Gaeta") [29] and the geophysical survey (tomography) performed in the area [28]. In this regard, the geological section AA' is shown in Figure 2.

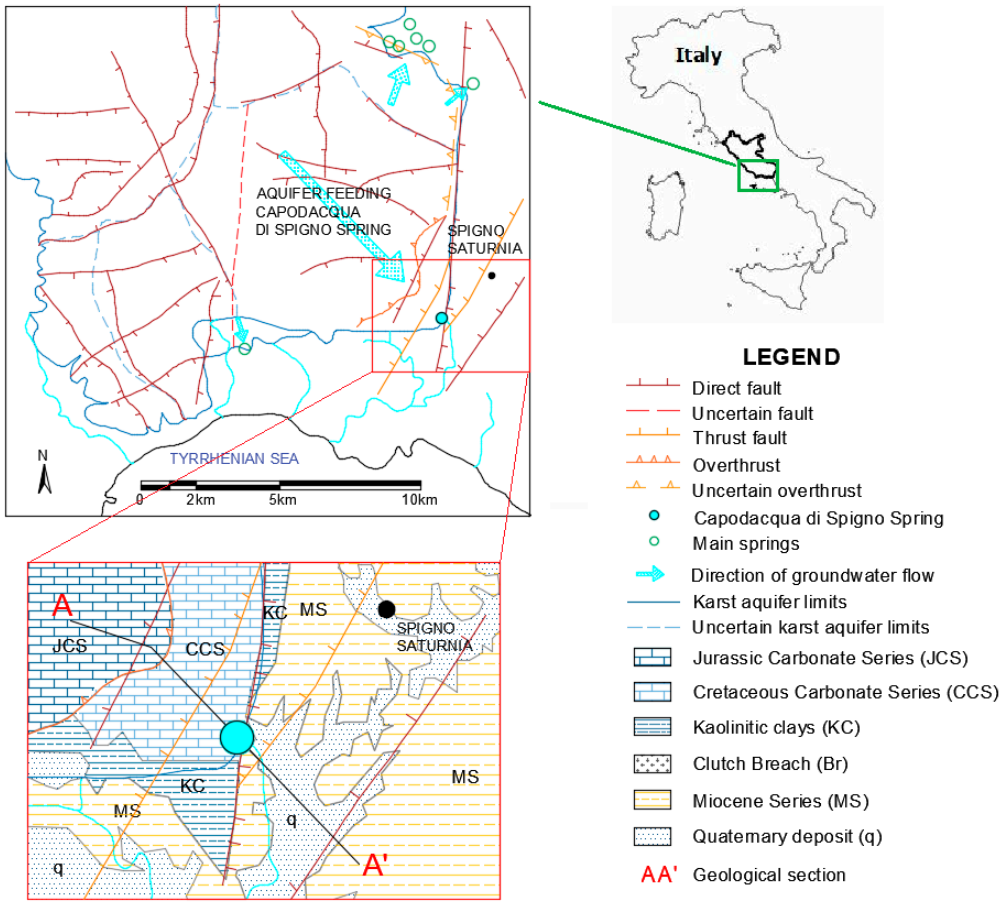

Figure 1. Structural map and main groundwater flow direction of Capodacqua di Spigno Spring (up); excerpt of the geological map and positioning of the geological section AA′ represented in Figure 3 (down)—based on Baldi et al., 2005 [28].

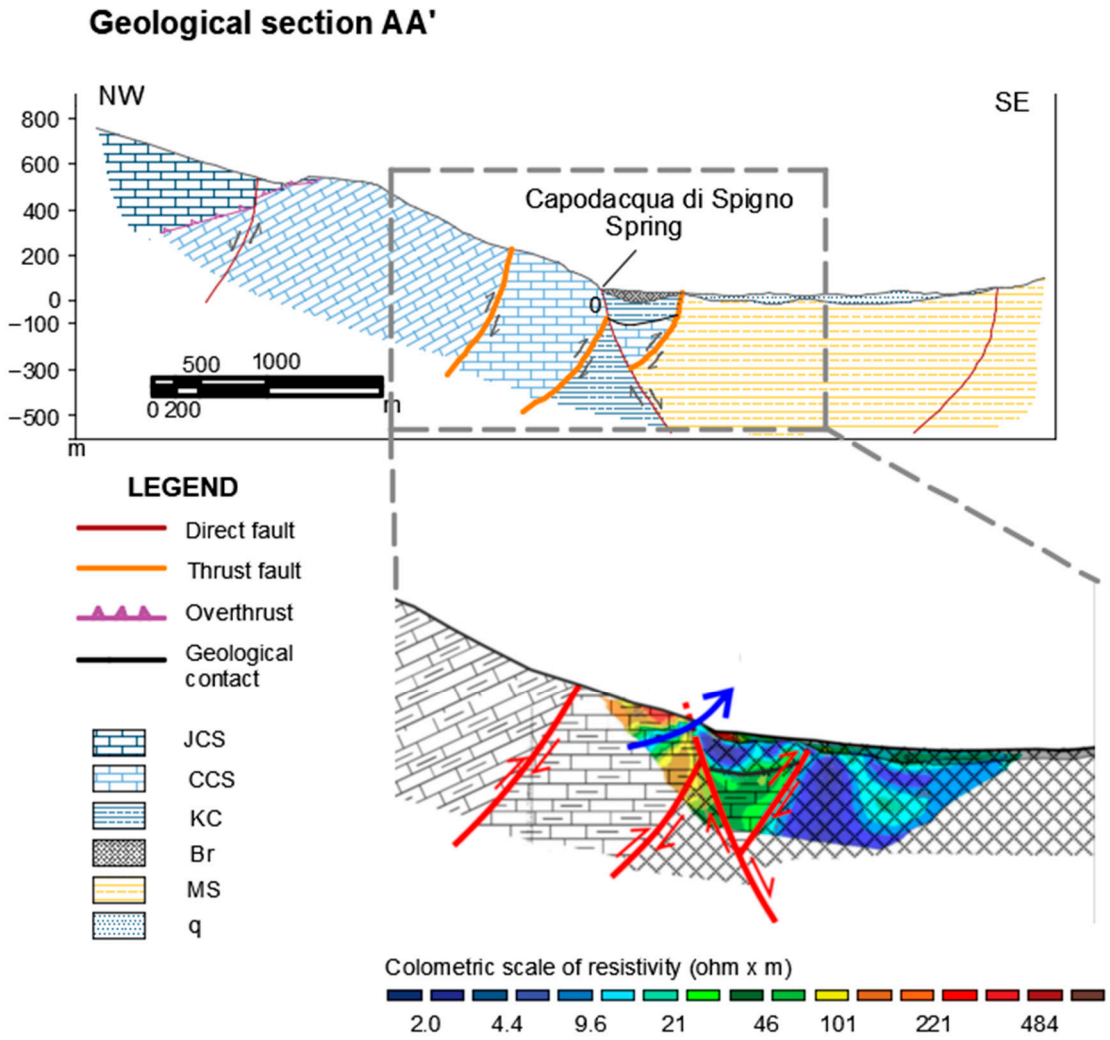

Figure 2. Geological section AA' (trace in Figure 1) modified from the study of the geological map of Italy [29] and geological map edited by Baldi et al., 2005 [28]: the image below depicts the structural pattern by geoelectric tomography interpretation. Legend: JCS is Jurassic Carbonate Series; CCS is Cretaceous Carbonate Series; KC is Kaolinitic Clays; Br is Clutch Breach; MS is Miocene Series and q is Quaternary deposits.

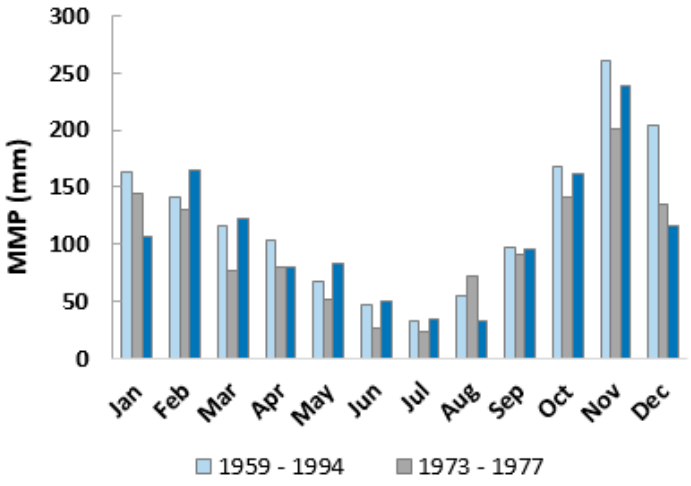

Figure 3. Mean Monthly Precipitation (MMP) seasonal trend in the study area, based on [26].

2.2. Climate Framework

Regarding the climate assessment of the study area, it has been evaluated on the basis of monthly rainfall time series collected in the "Esperia" rainfall gauge, the closest to the recharge area of the spring, in the northern part of the hydrogeological basin. However, rainfall values from 1994 to 2011 are not available for this pluviometric station. Therefore, the rainfall behavior for the longest time series available, i.e., from 1959 to 1994, was studied. The mean annual precipitation (MAP) of the time series ranges from 811 to 2103 mm/year in the period 1959–1994. The rainfall seasonal trend (Figure 3) shows that the most important contribution is due to the rainiest season (from November to February), with a trend inversion in the last eight years (2012–2020), where a deficit has been registered, mostly due to a reduced contribution of rainfall in January and a positive increase in February and March.

3. Materials and Methods

3.1. Data Collection

In addition to the 14 samples already analyzed, whose results have been previously published [21], the isotope geochemistry laboratory of the University of Parma (Italy) tested 10 more groundwater samples, which were taken always from Capodacqua di Spigno Spring. This means that we considered 70% more samples. The IRMS (Isotope-ratio mass spectrometry) continuous low-equilibration method, with CO_2 for $\delta^{18}O$ and H^2 for δ^2H, was applied. The results of all samples collected at the spring, shown in Table 1, are expressed as per mil deviations from the internationally accepted standard VSMOW (Vienna Standard Mean Ocean Water). The "¦Ä" notation is a way to express the relative abundances of oxygen (^{16}O, ^{18}O) and hydrogen (^1H, ^2H) isotopes in the water molecules [30]. The analytical error is ±0.2‰ for $\delta^{18}O$ and ±1‰ for δ^2H.

During the same time period the Department of Civil, Building and Environmental Engineering (DICEA) team took spring water samples and carried out discharge measurements. Specifically, the authors made measurements along the river downward of the spring to determinate the excess flow rate of the spring, which has to be added to the discharge, collected by the local water supply agency Acqualatina Spa, in order to obtain the total amount of the spring outflow, Qs, as represented in Table 1. Measurements were conducted by the application of traditional current-meter method [21]. The stream flow velocity was measured through a SEBA horizontal axis current-meter F1, according to EN ISO 748:2007 requirements. This activity consisted mainly of measuring the excess flow rate of the spring in a discharge channel [26]. The current meter measures velocity at a one point, so it requires determination of the mean velocity in each of the selected verticals. When possible, to measure water velocity, the "Three-Point Method" described by the "National Environmental Monitoring Standards (NEMS)" was used [31].

Table 1. Isotope composition of spring water ($\delta^{18}O$, $\delta^{2}H$), flow rates exploited by the local water supply (Qe), excess flow rates measured in the river (Qm) and reconstruction of the discharges supplied by Capodacqua di Spigno Spring (Qs), (new data in bold).

Date	$\delta^{18}O$ (‰ VSMOW)	$\delta^{2}H$ (‰ VSMOW)	Qe (l/s)	Qm (l/s)	Qs (l/s)
26 April 2018	−7.22	−40.09	520	915	1435
25 May 2018	−7.24	−40.35	506	780	1286
27 June 2018	−7.29	−41.02	537	490	1027
30 July 2018	−7.32	−41.07	543	251	794
29 August 2018	−7.27	−40.94	554	159	713
1 October 2018	−7.37	−41.20	489	168	657
8 November 2018	−6.91	−37.92	454	1657	2111
18 December 2018	−6.78	−37.57	486	2164	2650
18 January 2019	−7.14	−39.80	503	829	1333
19 February 2019	−7.23	−40.29	504	1050	1555
20 March 2019	−7.26	−40.58	454	837	1291
30 April 2019	−7.23	−40.09	433	558	991
29 May 2019	−6.74	−37.15	435	2500	2935
26 June 2019	−7.37	−41.22	458	671	1129
25 July 2019	**−7.36**	**−40.54**	**524**	**337**	**861**
29 August 2019	**−7.31**	**−40.47**	**534**	**102**	**636**
27 September 2019	**−7.40**	**−40.73**	**487**	**102**	**589**
30 October 2019	**−7.49**	**−41.60**	**466**	**52**	**518**
27 November 2019	**−6.43**	**−36.05**	**449**	**2242**	**2690**
23 December 2019	**−6.95**	**−39.00**	**425**	**3000**	**3425**
28 January 2020	**−6.76**	**−37.63**	**443**	**1440**	**1883**
27 February 2020	**−7.17**	**−39.80**	**450**	**784**	**1234**
28 April 2020	**−7.22**	**−39.86**	**417**	**595**	**1012**
25 May 2020	**−7.30**	**−40.54**	**421**	**550**	**971**

The morphometric parameters were defined by using the digital elevation model (DEM) discretized into finite square elements (FSE), with the size of 100 × 100 meters, using the open source software Q-GIS. In this way the elevation classes distribution of Capodacqua di Spigno basin was extracted. from the resampled DEM.

The value of the monthly supply volume of the aquifer was calculated through the inverse hydrogeological water budget method application [23–25]. For the average monthly groundwater recharge estimation (i.e., the effective infiltration), data referring to four meteorological stations near the study area, for a time series of 40 years (1959–1999) for rainfall and 6 years (2012–2018) for temperature, were used. The thermo-pluviometric stations are Gaeta, Itri, Esperia and Santi Cosma e Damiano, which cover an area of about 220 km^2 (Figure 4) [32].

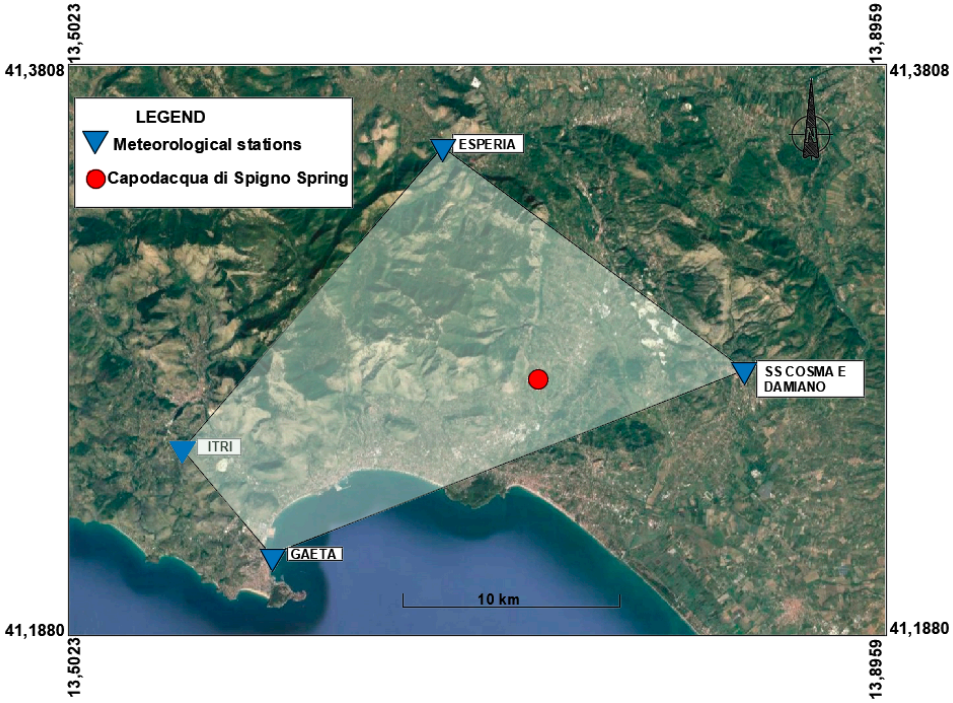

Figure 4. Thermo-pluviometric stations of the study area (latitude and longitude are in decimal degrees).

3.2. Average Recharge Areas Elevation (I-Elevation)

In a given hydrogeological basin, groundwater sources may be fingerprinted using isotopes, such as ^{2}H and ^{18}O, which depend on infiltration altitude of rainfalls. Higher infiltration altitude will have precipitations, which are depleted in ^{2}H and ^{18}O. The altitude effect is used in hydrogeological studies because it allows researchers to determine at which altitude recharge areas are located. However, some studies on this topic have emphasized that the value assumed by the gradient of isotopic content varies according to meteo-climatic characteristics, too [33]. In Italy, the average values of vertical isotopic gradient are given by $Grad^{18}O = -0.24‰/100$ m of elevation for $\delta^{18}O$ [12] and $Grad^{2}H = -1.8‰/100$ m of elevation for $\delta^{2}H$ [12]. Therefore, in this study, the average elevation values of the recharge area (I-elevation) were estimated starting from $\delta^{18}O$ and $\delta^{2}H$ values detected for Sabaudia Station (17 m a.s.l.) [11]. These values are computed by solving the following formulas:

$$\delta^{18}O_{Sab} + (Grad^{18}O \cdot \Delta q) = \delta^{18}O_{Spring}; \quad (1)$$

$$\delta^{2}H_{Sab} + Grad\ ^{2}H \cdot \Delta q) = \delta^{2}H_{spr}; \quad (2)$$

where:

$\delta^{2}H_{Sab}$ and $\delta^{18}O_{Sab}$ are the $\delta^{2}H$ and $\delta^{18}O$ values detected for Sabaudia Station;

$\delta^{2}H_{spr}$ and $\delta^{18}O_{spr}$ are the $\delta^{2}H$ and $\delta^{18}O$ values detected for the spring.

Considering that Δq = difference between the elevation value of the mean recharge area and the altitude of the Sabaudia station, it results that:

$$q_{^{18}O} = \frac{|\delta^{18}O_{spr} - \delta^{18}O_{Sab}|}{Grad^{18}O} + q_{Sab}; \quad (3)$$

$$q_{^{2}H} = \frac{|\delta^{2}H_{spr} - \delta^{2}H_{Sab}|}{Grad\ ^{2}H} + q_{Sab}; \quad (4)$$

where:

q_{Sab} is the Sabaudia station elevation (17 m a.s.l.)

$q_{^2H}$ and $q_{^{18}O}$ are the mean elevation values of the recharge area related to ^{2}H and ^{18}O;

Now it is possible to define q as the average elevation of the recharge areas between the mean elevation, respectively, related to ^{2}H and ^{18}O.

$$q = \frac{1}{2}(q_{^{18}O} + q_{^2H}) \quad (5)$$

3.3. Isotope-Driven Model

The isotope-driven model proposed by Iacurto et al. [21] is based on the assumption that the isotopic composition of spring water is mainly due to the elevation effect, linked to the topographic variation of the aquifer basin surface. This assumption suggests that the variation in the isotopic concentration of rainfall, given by meteo-climatic factors, is indifferent or has little influence on the spring isotope composition. In order to demonstrate the existence of this assumption, a preliminary check procedure is introduced. The latter must be used to define the influence of meteo-climatic factors (seasonal and amount effects) on the isotopic composition variability of the spring water.

3.3.1. Preliminary Check of the Rainfall Influence

In the area where the model is applied, a preliminary support study, which aims to define the degree of influence of the rainfall's isotopic variability on the spring's isotopic concentration, has to be performed. A check procedure has been set up with this aim, and it assumes that the isotopic concentration of the springs changes in relation to the input rainfall ones because of temperature changes (seasonality effect) and magnitude of rainfalls (amount effect). These meteo-climatic factors act in a discordant way on isotopic concentration of rainfall [34,35]. Thus, the isotopic enrichment is due to temperatures increasing as well as to rainfall intensity and duration decreasing. On the contrary, isotopic depletion occurs when temperatures decrease and rainfall intensity and duration become bigger. In addition, based on these natural trends, intense meteoric events in summer (in the Northern Hemisphere) produce rainfalls depleted in isotopic concentration in comparison to others more commonly seen in the same season [36].

With the aim of better taking in account all these factors, any range of distribution of considered parameters has been normalized, referring to the maximum and minimum registered value. As a consequence of this, we have introduced partial relative indexes:

- Temperature index:

$$\gamma_{i_{T20}} = \frac{\Delta T_{20_i} - \Delta T_{20_{min}}}{\Delta T_{20_{max}} - \Delta T_{20_{min}}} \quad (6)$$

where ΔT_{20} is the variation from 20 °C, which is usually defined as the mean condition (amount effect threshold) [36];

- Monthly rainfall index:

$$\gamma_{i_{Rm}} = \frac{R_{m_i} - R_{m_{min}}}{R_{m_{max}} - R_{m_{min}}} \quad (7)$$

where R_{m_i} is the monthly cumulative rain of the *i*-month (periodic rainfall amount), defined in terms of rain height.

- Forty eight hour rainfall index:

$$\gamma_{i_{R48h}} = \frac{R_{48h_i} - R_{48h_{min}}}{R_{48h_{max}} - R_{48h_{min}}} \quad (8)$$

where R_{48h_i} is the 48 h cumulative rainfall (rainfall event amount), defined in terms of rain height.

As temperature and rainfall magnitude act discordantly on isotopic concentration of rainfall, and considering as equal the influence of monthly rainfall and short rainstorm events, a combined rainfall isotopic index, *IR*, can be defined in the following expression:

$$IR_i = \left[\gamma_{i_{T20}} - \frac{\left(\gamma_{i_{Rm}} + \gamma_{i_{R48h}}\right)}{2}\right] \quad (9)$$

IR can assume values in the range [−1, 1] in relation to the isotopic depletion and enrichment effects influencing rainfall water, e.g., heavy rain in winter and drought in summer, respectively, define the aforesaid extreme conditions.

In the meantime, an IS index related to the isotopic concentration of the spring is introduced to compare it with IR. Thus, IS defines the isotopic enrichment and depletion in the range [−1, 1], such as IR, and for an i-th value of isotopic concentration of the spring IS has the following expression:

$$IS_i = 2\left[\frac{\delta^{18}O_i - \delta^{18}O_{min}}{\delta^{18}O_{max} - \delta^{18}O_{min}} - \frac{1}{2}\right] \quad (10)$$

For any further comparative analysis, it should be considered that the isotopic concentration of groundwater at the spring is the result of the infiltration of different rainfalls which have previously involved the aquifer basin. Starting from this assumption, an analysis has been performed to highlight the relationship between the isotopic concentration trend, represented by (*IS*), and the combined trend of the temperature and amount effects (*IR*) on the isotopic concentration of multimonth rainfalls. This last trend was therefore calculated by using the average values computed for different time intervals (1, 2, 3, 4 and 5 months), of $\Delta T_{20_i}, R_{m_i}, R_{48h_i}$. The time intervals are considered as lags from the month of spring water sampling.

3.3.2. The Model

By using the isotope-driven model [21], it was possible to identify the main recharge areas according to the variation of isotopic rates detected in groundwater samples taken at the spring. The model is based on the ascertained linear relationship between the spring discharges and the relative average recharge area elevations, I-elevation, detected by oxygen-18 and deuterium isotopes [21]. Specifically, the linear regression (Figure 5) suggests a main trend that associates I-elevation with an increase of the flow rate. In this way, other secondary effects, probably due to seasonality and impulsive/cumulate rainfall events influencing the isotopic concentration, are not considered in the model:

1. With the increase in the rainfall intensity without an increase in the recharge area involved, the flow rate changes but the average recharge area elevation remains invariant;
2. The same rainfall intensity involves different recharge areas; the flow rate remains invariant while the average recharge area elevation changes.

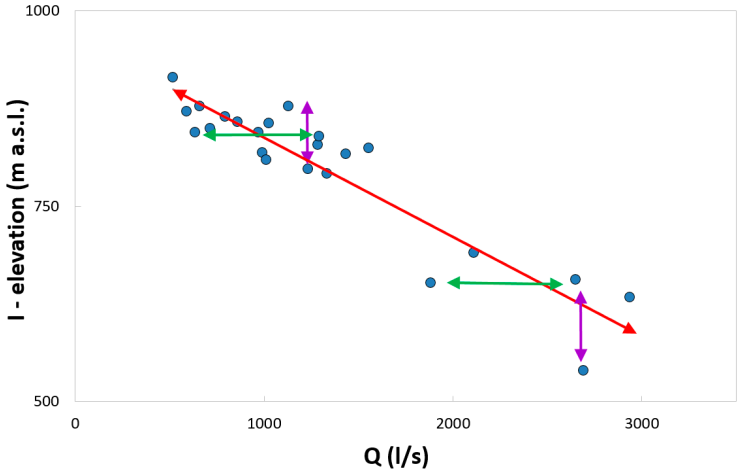

Figure 5. Conceptual model: higher flow rates associated with higher recharge areas, involving lower altitude areas (red arrow). Secondary behaviors: different flow rates associated with the same average recharge area elevation (green arrows); same flow rate associated with different average recharge area elevations (purple arrows).

With the aim of linking the single flow rate value to only one recharge area value, linked in turn to one value of average altitude, we introduced the equivalent geometric area (A_{eq}) [21]. This equivalent area is therefore calculated in terms of the weighted average of the elevation classes, as described by the following formula.

$$A_{eq} = \frac{\sum_1^n (A_i \cdot h_i)}{\sum_1^n (h_i)} \quad (11)$$

where Ai is the area related to i_{th}-elevation h_i.

In the model, it is considered that the maximum discharge of the time series is associated with the total topographic elevation distribution of the area, as wholly involved in the recharge. It is possible to assume that:

$$A_{eq} = A_{eq\_max} \quad (12)$$

The topographic average elevation is therefore defined as:

$$h_{top} = h_{eq\_max} = \frac{\sum_1^n (A_i \cdot h_i)}{\sum_1^n (A_i)} \quad (13)$$

where h_{top} and h_{eq_max} are, respectively, the topographic average elevation and the average recharge area elevation associated with the maximum discharge.

In addition, considering the inverse linear relationship between the average recharge area elevations and the spring discharge values, it is possible to assume that the minimal value of spring discharge is associated with a smaller equivalent recharge area (A_{eq_min}). This has a higher elevation (average recharge area elevation) detected by isotopic ratio values. A_{eq_j} is the generic equivalent recharge area associated with the generic j_{th}-discharge, which corresponds to an average elevation h_{q_j}, obtained by isotopic concentration values.

$$A_{eq\_j} = \frac{A_{eq\_max} \cdot he_{q\_max}}{h_{eq\_j}} \quad (14)$$

In this way, the analytical model identifies the recharge area associated with j_{th} discharge as a minor quantity of the total aquifer area. The recharge area is redistributed across the real aquifer through the Weibull cumulative probability function [37], starting with covering the highest altitudes (Figure 6).

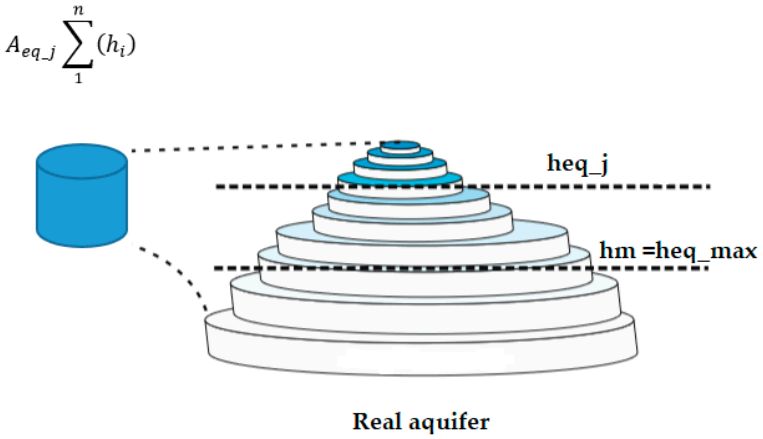

Figure 6. Representation of the recharge area redistribution model on the real topographic surface, starting from the top of the relief. This area refers to the equivalent regular aquifer dependent from flow rate (Equation (3)). The non-uniform redistribution was made using the Weibull cumulative probability function (Equation (4)), with the aim to detect the recharge area involved in the real aquifers.

The model uses the two parameters for the calibration of Weibull function (k and λ), these are found by iterative process; up to satisfy the following condition:

$$A_{eq\_j} = A_{eq\_weibull} \rightarrow \frac{A_{eq\_max} \cdot he_{q\_max}}{h_{eq\_j}} = \frac{\sum_1^n A_i \left(1 - e^{-\left(\frac{h_i}{\lambda}\right)^k}\right) h_i}{\sum_1^n (h_i)} \quad (15)$$

where:

$A_{\_(eq\_weibull)}$ is the weighted average area computed using the Weibull function;

h_i is the central value of the class elevation associated with the topographic i_{th}-class area A_i;

k and λ, respectively, are the shape and scale modelling parameters of the Weibull function. In this specific model, their behavior shows that k has a regular non-linear decrease with discharge and a regular non-linear decrease with elevation; while λ has a regular non-linear increase with elevation and a regular non-linear decrease with discharge.

As previously mentioned, the new version of the isotope-driven model includes integrations based on meteo-climatic data analysis, as shown in Figure 7.

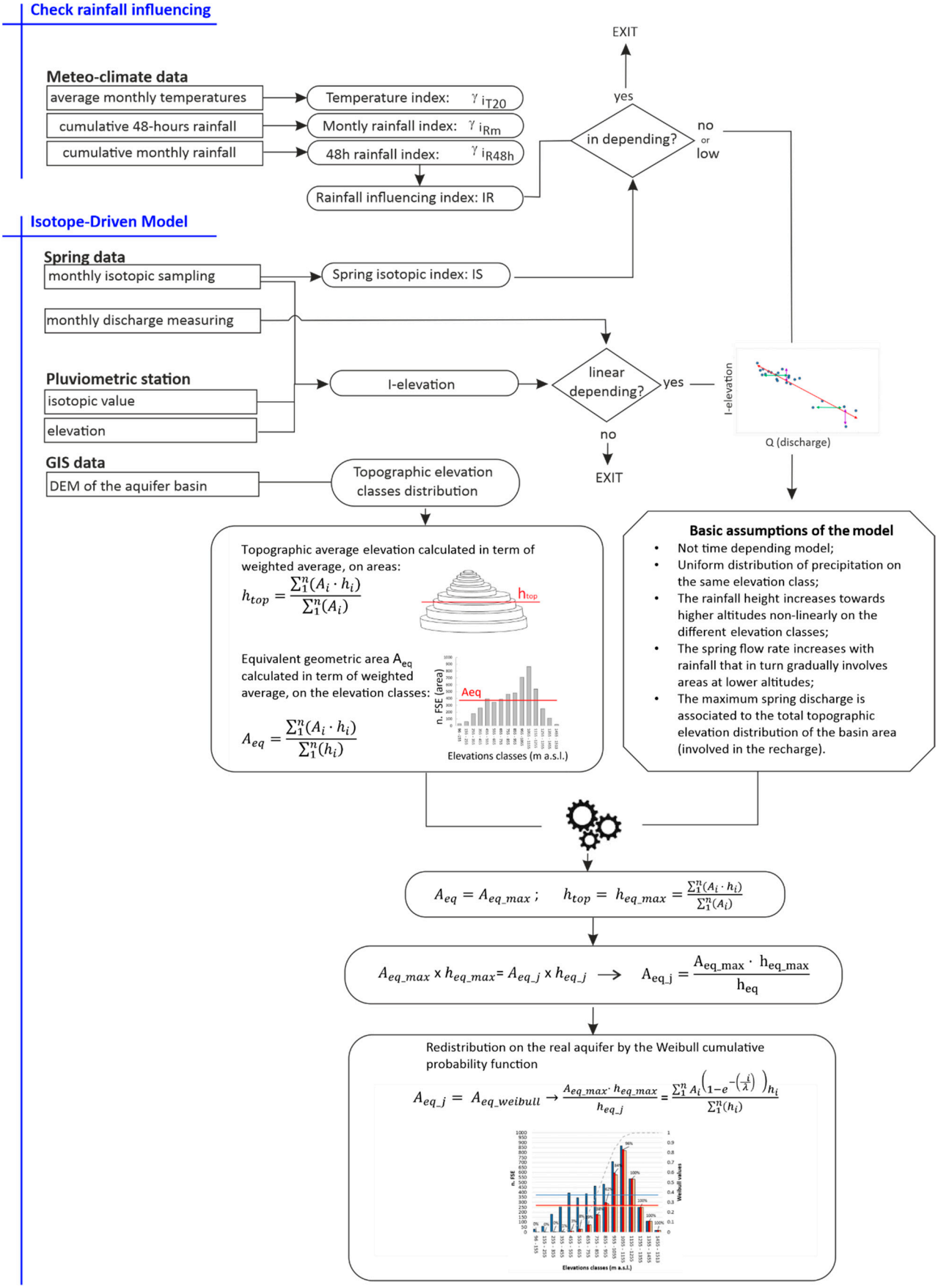

Figure 7. Flowchart of the proposed procedure for the recharge area estimation.

4. Results

4.1. Oxygen-18 and Deuterium Isotopes Analyses

Figure 8 shows the oxygen-18 and deuterium ¦Ä values for Capodacqua di Spigno Spring together with the Global Meteoric Water Line (GMWL), the Mediterranean Meteoric Water Line (MMWL) and two local meteoric water lines for central Italy, i.e., the two Central Italy Meteoric Water Lines (CIMWL) [11,12].

The graph reported in Figure 8 highlights what was found in the first phase of monitoring and isotopic analysis of the waters of Capodacqua di Spigno Spring [21], i.e., the variation in the isotope values is connected to the variation in the spring flow rates. When Capodacqua di Spigno spring delivers maximum flow rates, $\delta^{18}O$ and δD change and become enriched in ^{18}O and ^{2}H.

The altitude and (to a lesser extent) the latitude are the main geographical factors affecting the isotopic signature of precipitation in Italy [12]. Considering that in this case we are analyzing the isotopic content changes within the same study area, such a change is mainly due to the altitude–topographic effect. As for the effect of seasonality on groundwater, the enrichment in both heavy isotopes of meteoric waters is irrelevant in the warm months. In fact, for Capodacqua di Spigno Spring, in the warm months (Figure 8) the water show lesser δ-values than in the others. In this regard Figure 8 shows that spring waters have a general δ-values trend characterized by a poor or discordant relationship with the seasonal effect characterizing the rainfall water, encountered by P. Bono et al. [38] in a coastal area about 100 km away from Capodacqua di Spigno. In fact, at this spring dry months result in a greater heavy-isotope enrichment compared to the other warm months and vice versa. Therefore, the seasonal effect influences the variation in the isotopic content in the rainfall water, but is not evident in groundwater [10]. This is due to the fact that groundwater is the storage water coming from several rainfall events, which occurred over the course of several months. Additionally, with regard to the so-called amount effect, the isotopic values of the spring waters seem to have a discordant trend with what usually occurs in rainwater. In fact, in the rainy months, the rainwater is characterized by the depletion of isotopes [34–36], contrary to what was found in Capodacqua di Spigno Spring. The wettest months, in the case study, are in fact the winter ones, as well as the month of May 2019, which are characterized by spring waters being more enriched in heavy isotopes than during the driest months (Figure 8). However, the main trend common to all values depends on the variation of the infiltration altitude. Actually, as expected, the altitude–topographic effect has a relevant role in the mountain areas.

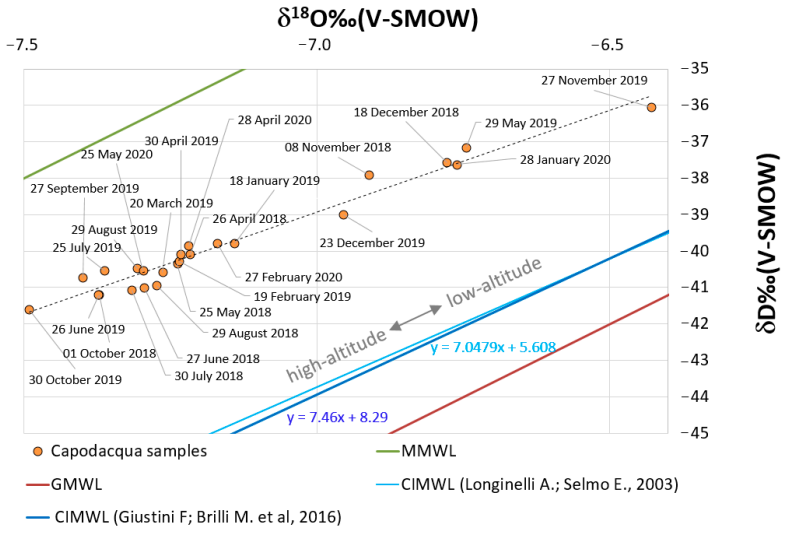

Figure 8. Plot of $\delta^{2}D$ vs. $\delta^{18}O$ for Capodacqua di Spigno samples.

The spring water samples collected on 29 May 2019, 18 December 2018 and on 28 January 2020, regarding the events of maximum flow rate, show similarly high content of heavy isotopes. This occurred despite the different rainfall regime and season that characterized these three events. Therefore, this effect can be mainly attributed to the "altitude effect", i.e., to the infiltration of the precipitation at a lower elevation than the water collected in all the other samples. If the altitude effect is considered to be predominant, the samples that appear to be more depleted in heavy isotopes are those associated with a higher average recharge elevation. These samples were collected during spring, in the months when the spring flow rate was lower. In this regard, it is possible to affirm that the isotopic variation of the spring depends on the flow rate rather than on rainfall seasonality.

4.2. Isotope-Driven Model Analyses

4.2.1. Rainfall Influence

About the case study, Figure 9 shows that the spring isotopic variability curve, represented by IS, is lowly correlated or opposed to IR that represents the variability of the meteo-climatic factors influencing the rainfall isotopic ratio. This effect is observed both considering the month of spring water sampling (1 month) and up to four previous months. In observation of the scope of the introduced check procedure, this condition is in favor of the topographic effect (altitude effect) as the main factor characterizing the water isotopic concentration of the spring. Besides, this condition meets the behavior already observed at the extremes of the series. The evidence is in the fact that the higher isotopic concentrations (isotopic enrichment) in the spring water are related to the greater rainfall magnitudes that occurred in the cold periods prior to sampling; e.g., 27 November 2019 and 18 December 2018. Different and significant is the minimum related to the 30 October 2019, in proximity to the maximum, which occurred at about the same temperature but in a period with very low rainfall. In addition, it seems that the rainstorm events (cumulate at 48 h) have a remarkable inverse correlation with the isotopic enrichment peak measured at the spring (e.g., 29 May 2019).

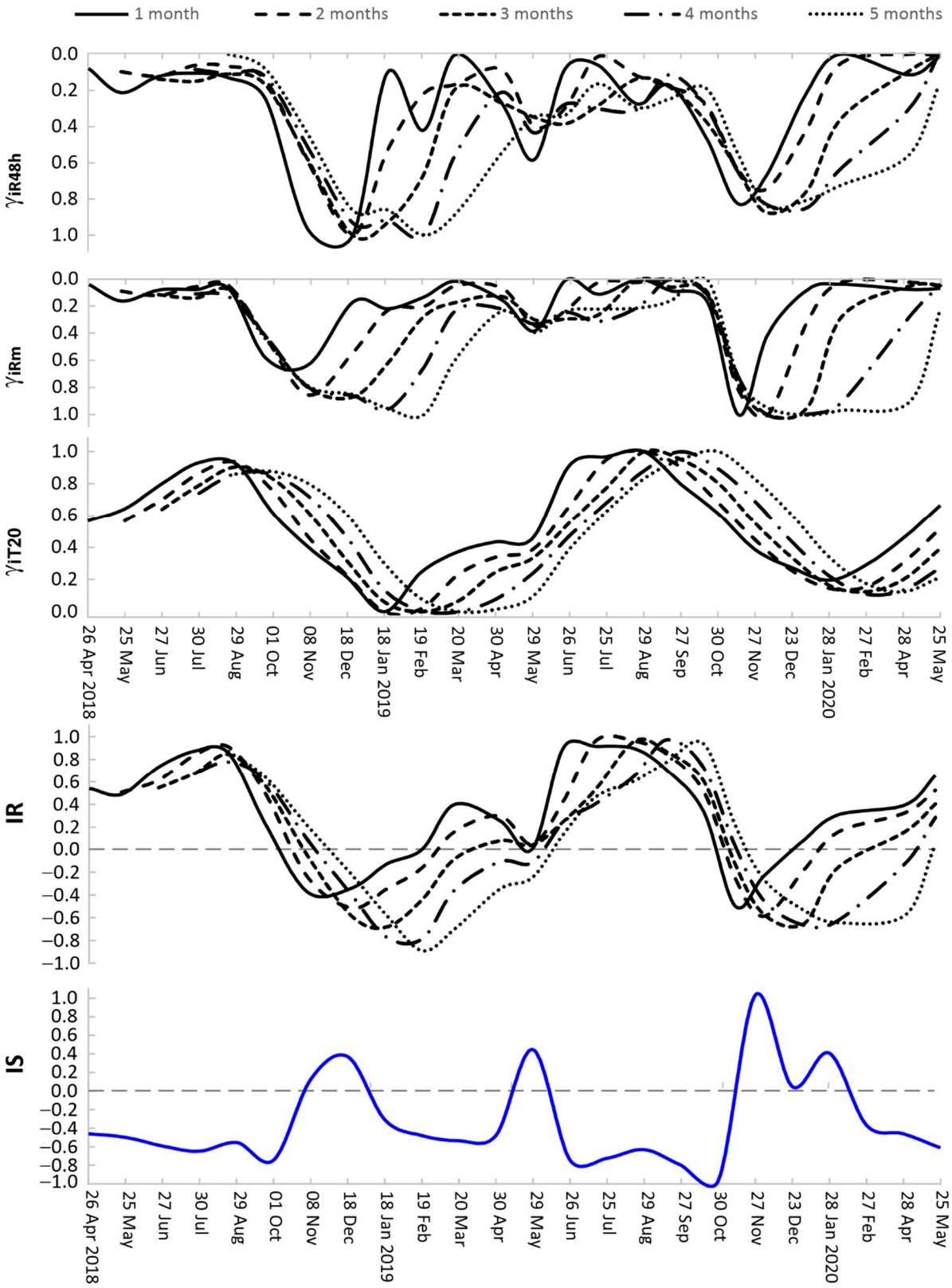

Figure 9. Trend of the partial indices: 48h Rainfall Index ($\gamma_{i_{R48h}}$); Monthly Rainfall Index ($\gamma_{i_{Rm}}$); Temperature Index ($\gamma_{i_{T20}}$). Trend of the combined rainfall isotopic index (IR) and trend of the index related to the isotopic concentration of the spring (IS)—1 month = month of spring water sampling, 5 months = from the same month up to 4 months prior to sampling.

4.2.2. Recharge Areas

The spring discharge values, measured on the same days as the spring water sampling, were compared with the average elevation values of the recharge area, I-elevations, obtained using the oxygen-18 and deuterium isotopes (Figure 10).

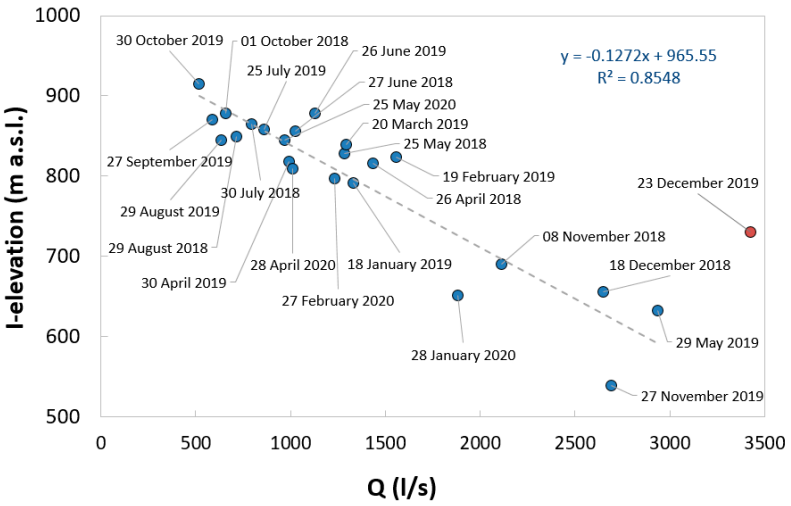

Figure 10. Update of the linear relationship proposed in the previous paper [21]**:** discharges supplied by Capodacqua di Spigno Spring in relation to average recharge area elevations.

In December 2019, extraordinary rainfall events occurred, which on 23 December 2019 caused the river to overflow, flooding of the surrounding area (Figure 11). It was therefore not possible to access the usual groundwater sampling point (drainage room). However, water was sampled from a different point (water fountain), where water extracted from the Capodacqua di Spigno Spring water comes directly out. This sample (red dot in Figure 10), as expected, is different from the main trend and can be considered an outlier due to the different sampling point. Indeed, in post processing analysis we realized that we sampled with the same modality performed in the drainage room. This state was not permitted to obtain an adequate purging of the pipe, considering that the water fountain is rarely open and it is quite far from the spring. With a good probability, the water stored had an isotopic concentration different from the water in the spring.

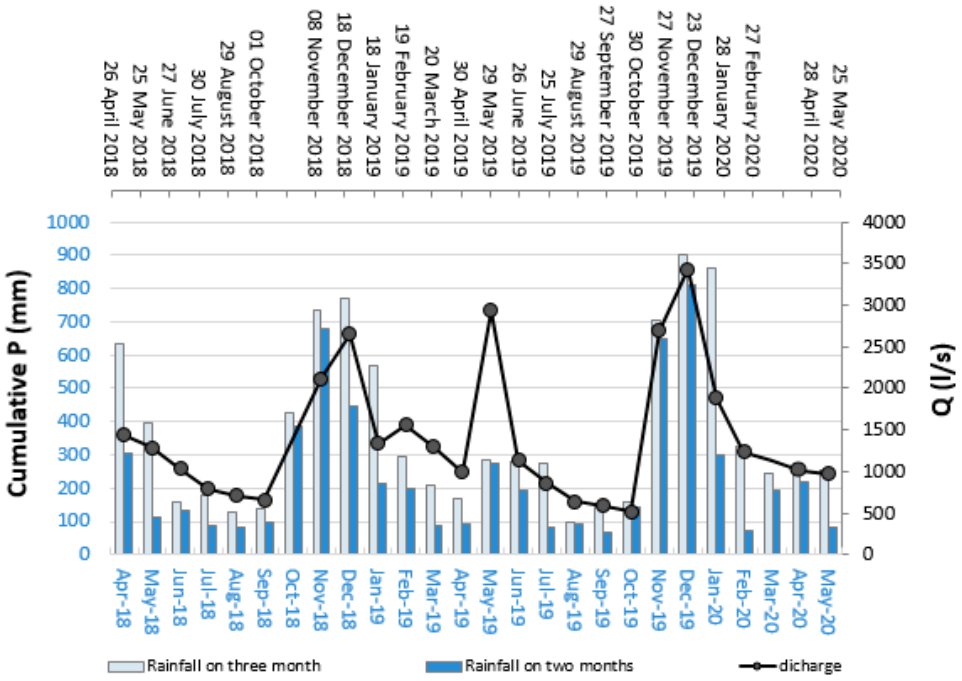

Figure 11. Comparison between spring discharge values (Q) and monthly cumulative rainfall data (Esperia Pluviometric Station, 302 m a.s.l.). Above the graph are the discharge sampling dates.

In reference to the previous values at the base of the isotope-driven model, the new isotopic vs. discharge values confirm the linear relationship between the spring discharges and average recharge area elevations detected by isotopic concentration [21]. This condition admits that the recharge area increases with the maximum flow rates of the spring; in this way their average elevation moves down, and vice versa. In addition, the assumption at the base of the model is that the recharge area associated with the maximum flow rate involves the whole area with higher elevation than the spring point. In this regard, as written in Equation (13), the topographic average elevation is set equal to the average recharge area elevation associated with the maximum discharge. The average recharge area elevation associated with the maximum discharge in May 2019 is similar to that of December 2018. Differently, the maximum discharge occurs in November 2019 gives a lesser I-elevation than this latter. This condition, which was probably effected by extraordinary 48 h rainfall event (Figure 9), was caused by a great runoff on the basin surface that shifted the infiltration at lower elevations. On the contrary, rainfall events more distributed over time are not characterized by great runoff on the topographic surface and therefore do not lead to a lowering of the average recharge area elevation. However, this lesser I-elevation does not produce substantial change in the slope of the I-elevation vs. discharge regression line (Figure 10). This condition permits us to use the isotopic driven model proposed in the previous study [21].

Starting from the elevation classes distribution of the topographic surface of Capodacqua di Spigno Spring basin, it was possible to apply the isotope-driven model to simulate the spring recharge areas. Figure 12 shows the recharge area distribution related to the maximum discharge (total area of the basin) and the recharge areas' distributions related to the two minimum discharges of 2018 and 2019, simulated by a model with a Weibull function.

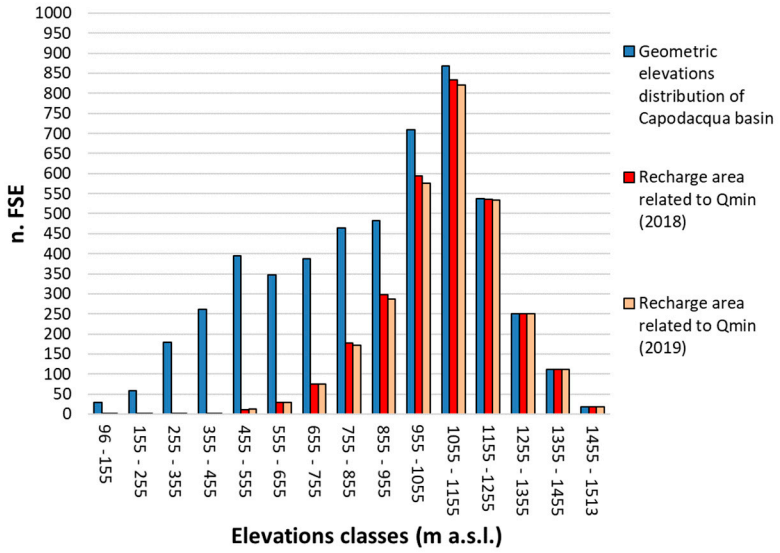

Figure 12. Recharge areas distribution simulated by the model defined by Iacurto et al. [21].

4.3. Estimation of the Aquifer Monthly Supply Volume

With the aim of having a hydrological validation of the isotope-driven model, a comparison was made between the estimated recharge areas, with the aforesaid model, and the monthly variability of the infiltration volume. This comparison was possible in that the monthly average recharge (monthly infiltration amount) of the Capodacqua di Spigno basin was distributed across the areas identified by different elevation classes.

The monthly average infiltration in the Capodacqua di Spigno basin has been evaluated, using the empirical method for estimating potential evapotranspiration (PET) proposed by Thornthwaite (1948) [22] applied to the inverse hydrogeological budget method (IHBM) [23–25]. The equation only requires mean monthly air temperature and mean daily daylight hours for each month, which can be calculated based on the latitude at the site of interest. With the aim of estimating the average monthly recharge of Capodacqua di Spigno basin, it was necessary to calculate the real monthly evaporation (RET), starting from potential monthly evapotranspiration (PET). For each cell, we compared the rainfall, through the rainfall–altitude relationships, with the PET. The real monthly evaporation was made equal to potential monthly evaporation if the rainfall value was bigger of the PET value, while the real monthly evaporation was imposed as equal to rainfall value if the rainfall value was less than the PET value.

First, the annual heat index (i), for each of the four rainfall stations (Figure 4) was calculated, so in the calculation of the potential evapotranspiration (PET) the average of the four annual heat index values was used (I_{mean}). In this regard, a summary table of the calculated values, necessary to estimate the PET of Thornthwaite, for each cell of the grid, is reported below (Table 2).

Table 2. Monthly Thornthwaite heat index (i), annual heat index (I), annual mean heat Index (Imean) and α coefficient for Capodacqua di Spigno basin.

	SS Cosma e Damiano	Gaeta	Itri	Esperia
$i_{January}$	2.10	2.96	2.14	1.81
$i_{February}$	2.54	3.22	2.33	2.24
i_{March}	3.55	4.26	3.41	3.50
i_{April}	4.96	5.64	4.71	5.04
i_{May}	6.65	7.40	6.34	6.73
i_{June}	9.51	10.13	9.24	9.81
i_{July}	10.94	12.01	11.04	11.83
i_{August}	11.35	12.45	11.45	12.19

$i_{September}$	9.03	9.94	8.61	8.76
$i_{October}$	6.91	7.84	6.76	6.50
$i_{November}$	4.63	5.48	4.48	4.08
$i_{December}$	2.43	3.46	2.81	2.19
I	74.60	84.78	73.33	74.69
I_{mean}		76.85		
A		1.86		

Regarding the four meteorological stations abovementioned, the average monthly rainfall module (A.M.R.M.), for the time series 1959–1999, and the average monthly temperature (A.M.T.), for the time series 2012–2018, were calculated. From the calculated values (A.M.R.M. and A.M.T.) it was possible to obtain the rainfall–altitude and temperature–altitude relationships for each month (Figure 13). For the rainfall–altitude and temperature–altitude relationships, linear interpolation has usually been used [24]. However, in the case of mountain basins, a logarithmic or exponential rainfall–altitude relationship leads us to obtain much more plausible values for the higher altitudes [32,39].

In this way, it was possible to estimate, for each finite square element (FSE), the value of the monthly potential evaporation (PET) and the real monthly evaporation (RET).

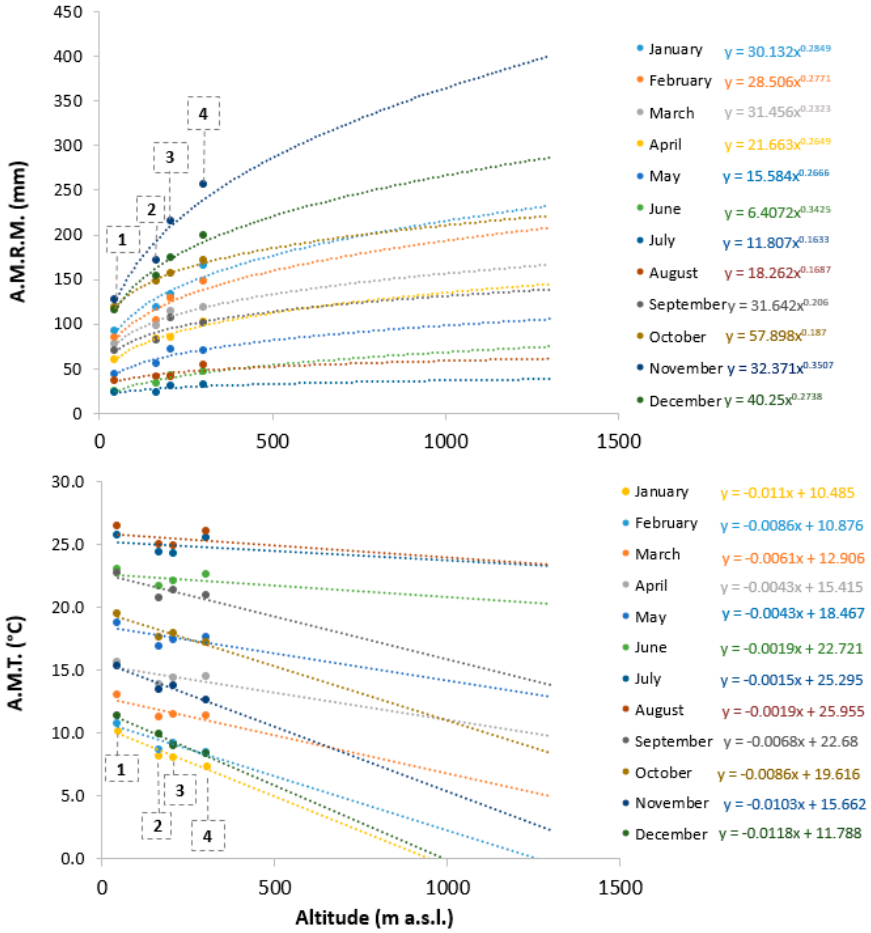

Figure 13. Rainfall–altitude relationship (top) and temperature–altitude relationship (down), for each month of the year. The thermo-pluviometric stations are: 1—Gaeta (45 m a.s.l.); 2—Itri (165 m a.s.l.); 3—SS. Cosma e Damiano (206 m a.s.l.); 4—Esperia (302 m a.s.l.).

By multiplying the single FSE infiltration value by the value of its area it was possible to obtain the average monthly infiltration volume (monthly average recharge). Figure 14

shows the estimation of the aquifer's monthly average recharge (M.A.R.) for each month of the year.

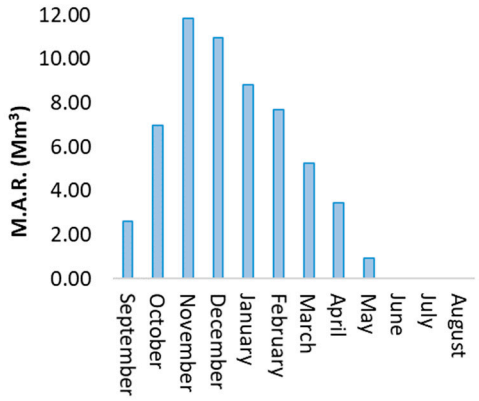

Figure 14. Monthly average recharge (M.A.R.) of Capodacqua di Spigno basin.

Figure 15 shows the distribution of the average recharge volume (M.A.R.) in the different months of the year. In Figure 15 it is evident that November (line blue) is the month with the highest infiltrated volume. In this month the recharge volume increases with the altitude, according to the rainfall–altitude relationship, based on the area available at each altitude. On the other hand, in May (line red), which, except for months with no infiltration, is the month with lowest infiltrated volume, only part of the basin is involved in the infiltration process. At low altitudes, in fact, the infiltration volume is zero. This is in accordance with the findings of the model, i.e., with the estimate of the recharge areas' distribution associated with the minimum and maximum flow rates (Figure 12).

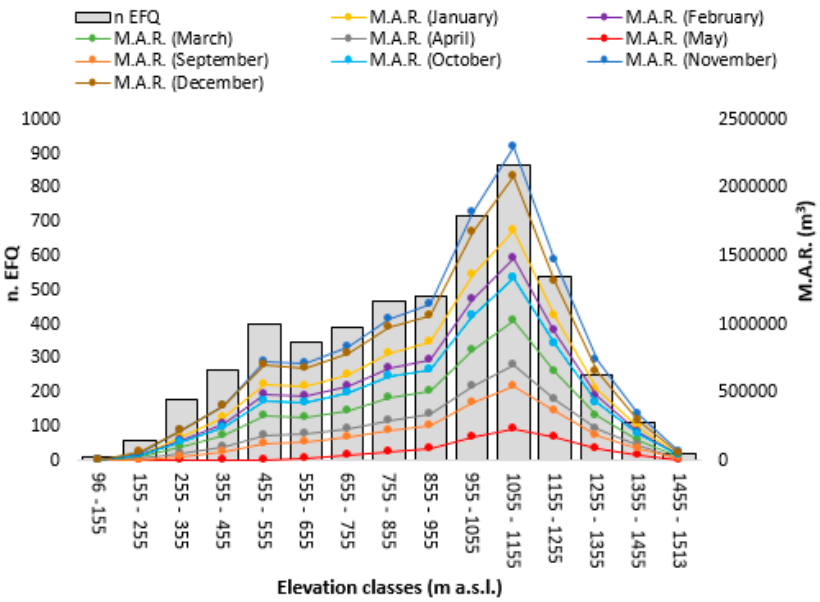

Figure 15. Monthly average recharge (M.A.R.) distribution of the different months on elevation classes of Capodacqua di Spigno basin (June, July and August are absent because they have zero infiltration); and elevation classes' distribution of Capodacqua di Spigno basin in terms of topographic surface (in grey).

Regarding Capodacqua di Spigno Spring, in a previous study the cross-correlation coefficient (C_{PiQ}) between the monthly spring discharge series and monthly rainfall series was analyzed [26]. C_{PiQ} numerically indicates how much each single previous monthly

rainfall value influences the total spring flow rate in relation to the specific month considered. For Capodacqua di Spigno Spring, the highest values of the correlation coefficients are from the same month up to four previous months (from i=0 to i=3) with respect to the spring flow rate occurrence. Considering that the minimum flow rate of the Capodacqua di Spigno Spring usually occurs between the end of August and mid-September, it can be assumed that the minimum discharge is mainly due to the infiltrations that occurred in the months of May, June, July and August. Therefore, it is possible to state that the minimum flow rate of the spring comes mainly from the infiltration that takes place in May, since the infiltrations of the months of June, July and August are equal to zero (Figure 14).

We therefore confirm what was simulated by the isotope driven model. It means that the recharge area associated with the minimum discharge is smaller and includes areas at higher altitudes. As a matter of fact, the graph in Figure 16 shows how the infiltration volume increases according to recharge area, since all the altitudes of the basin are affected by the infiltration.

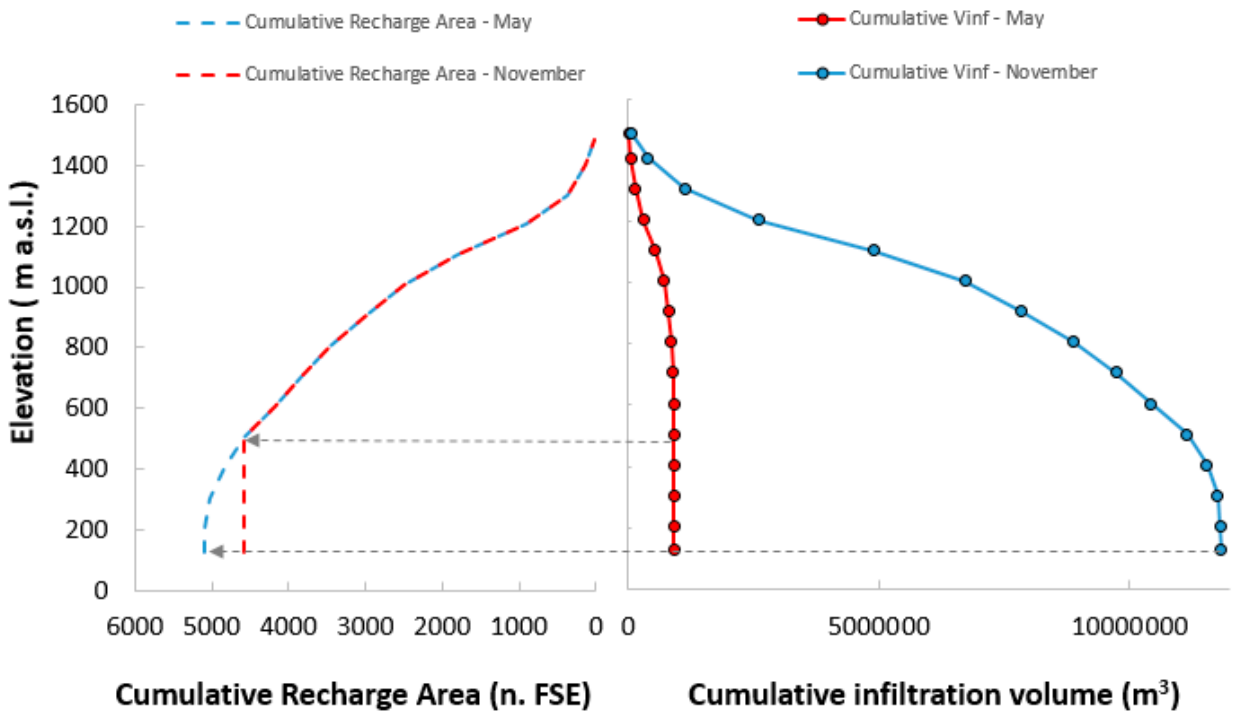

Figure 16. Cumulative recharge area of May and November on elevation (left); cumulative infiltration volume of May and November on elevation (right).

4.4. Isotope-Driven Model vs. Hydrogeological Budget Applications

Using an open source GIS plugin (GEarthView) it was possible to represent the results described above on Google Earth with the images presented in Figure 17. These figures show the simulated area involved by the infiltrations of May, identified by the inverse hydrogeological balance, and the recharge area related to Q_{min} carried out by the isotope driven model, respectively. It is quite evident that the two areas are very similar: they are smaller than the total surface of the Capodacqua di Spigno basin and involve only the highest altitudes.

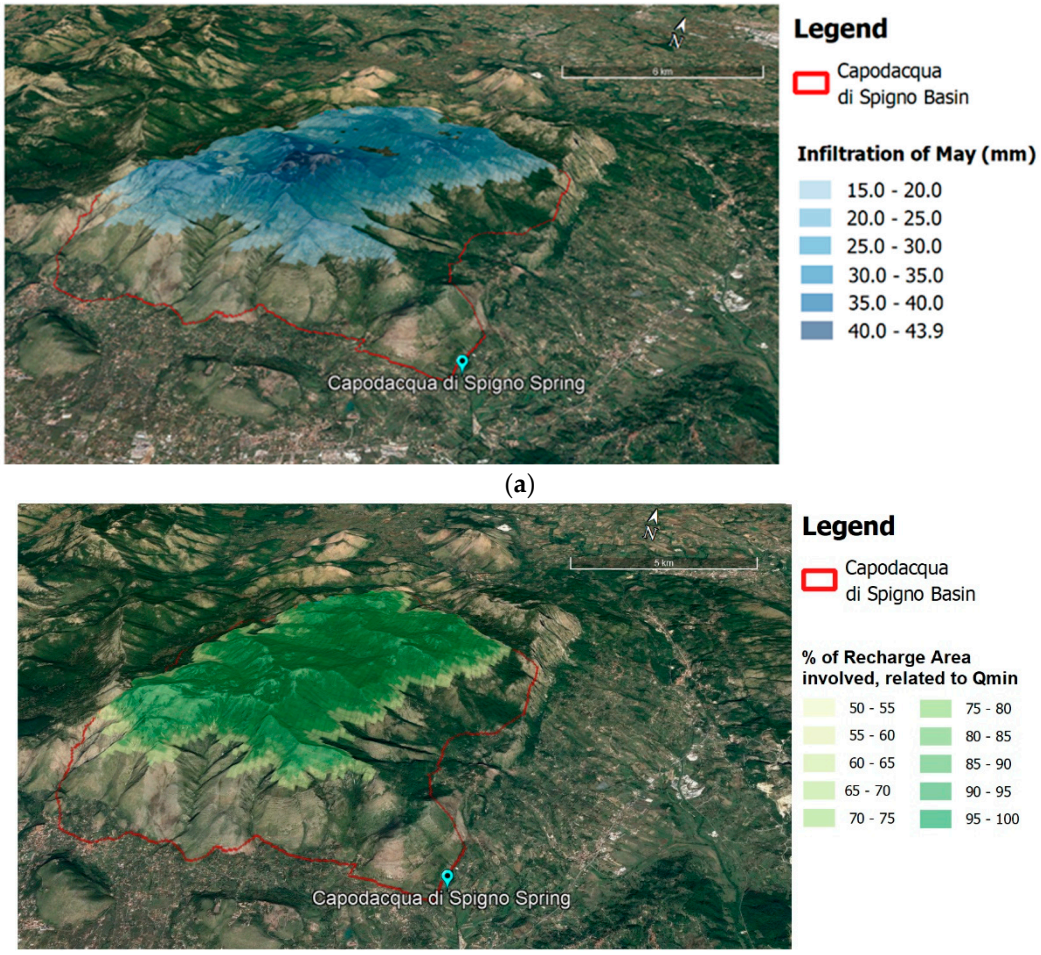

Figure 17. (**a**) Infiltration distribution of May (month of infiltration related to the minimum spring flow rate), by using the inverse hydrogeological balance [23]; (**b**) % of recharge area involved related to Qmin (2018), by using the isotope driven model [21].

5. Discussion and Conclusions

The isotope-driven model, set up with the aim of reaching a reliable means of identifying aquifer recharge areas, turned out to be a powerful tool, as this target is very important in several studies addressing groundwater protection. In this paper the isotope set up model presented in a previous paper [21] has been improved with a preliminary check procedure. This procedure is an important supplement to the model. This aims to compare the trend of the possible natural factors that influence the isotopic concentration of rainfall with the trend of the spring's isotopic concentration. In relation to these trends, a discordance or absence of correlation permits us to assume the elevation effect as predominant in the spring waters, and so the "isotope-driven model" can be run.

Several of the isotope-based techniques involve interpreting differences between the isotopic compositions of rainfall and groundwater samples [10,40,41]. However, in this paper, the preliminary check procedure analyses how the single affecting factor (seasonal and amount effect) that leads the variability of the rainfall's isotopic composition can influence the isotopic composition of the spring waters. In karst mountain aquifers, it is well known that the altitude effect is predominant compared to the other effects on spring's isotopic composition, and allows us to define the average recharge altitude [12,17,42]. However, this does not provide an indication of the recharge area. In this regard, the proposed model estimates the main recharge areas that feed the different spring discharges during the hydrological year.

The model has also been strengthened by the updating of new ^{2}H and ^{18}O data, with respect to the previous one [21], so it was possible to verify its soundness. Indeed, the 10

more spring water samples have made it possible to apply the model on a more extended isotopic dataset. This allowed us to analyze several maximum and minimum annual flow rates conditions.

On the other hand, as the application of tracers to groundwater characterization is generally preferable in a multitracing approach framework, in this case the set up model has been validated by a quantitative hydrogeological tool. It means that it has applied the Inverse Hydrogeological Budget method, modified for a monthly scale application, with the aim of finding the distribution of the mean infiltration volume in each area. Specifically, the monthly infiltration amount was distributed on the areas identified by different elevation classes. In this way, the minimum recharge areas identified with the isotope-driven model were compared with the monthly infiltration areas of those months related to the minimum spring flow rate. The research highlights that the distribution of the recharge areas on elevation classes given by hydrological water balance is very similar to the one resulting from the application of the isotope-driven model. Specifically, the application of the hydrogeological balance has confirmed that the total area of the basin is not always involved in the recharge process throughout the hydrological year. In dry periods, there is no infiltration in low altitude areas. In fact, considering May–August, i.e., the 4 months preceding the minimum flow rate of the spring, the corresponding recharge area is not the whole basin. This leads, in mountain karst basins such as the Capodacqua di Spigno one, to an increase in the average recharge altitude, which affects the isotopic values found in the spring water. The proposed model, which uses groundwater's isotopic signature, can be a preliminary tool for estimating the infiltration area and, therefore, improving the protection management of the aquifer, in reference to possible contamination sources affecting the feeding area.

Author Contributions: Conceptualization, G.S., S.I. and G.G.; methodology, G.S., S.I., G.G., F.M.D.F.; validation, G.S.; investigation, S.I., F.M.D.F.; data curation, S.I. and G.G.; writing—original draft preparation, S.I and G.G.; writing—review and editing, G.S. and F.M.D.F.; supervision, G.S.; project administration, G.S. All authors have read and agreed to the published version of the manuscript.

Funding: This research received no external funding.

Institutional Review Board Statement: Not applicable.

Informed Consent Statement: Not applicable.

Data Availability Statement: Not applicable.

Conflicts of Interest: The authors declare no conflict of interest.

References

1. Fatchurohman, H.; Adji, T.N.; Haryono, E.; Wijayanti, P. Baseflow index assessment and master recession curve analysis for karst water management in Kakap Spring, Gunung Sewu. *IOP Conf. Ser. Earth Environ. Sci.* **2018**, *148*, doi:10.1088/1755-1315/148/1/012029.
2. Goldscheider, N.; Chen, Z.; Auler, A.S.; Bakalowicz, M.; Broda, S.; Drew, D.; Hartmann, J.; Jiang, G.; Moosdorf, N.; Stevanovic, Z.; et al. Global distribution of carbonate rocks and karst water resources. *Hydrogeol. J.* **2020**, doi:10.1007/s10040-020-02139-5.
3. Sappa, G.; Iacurto, S.; Ferranti, F.; De Filippi, F.M. Groundwater quality assessment in a karst coastal region of the West Aurunci Mountains (Central Italy). *Geofluids* **2019**, doi:10.1155/2019/3261713.
4. Filippini, M.; Squarzoni, G.; De Waele, J.; Fiorucci, A.; Vigna, B.; Grillo, B.; Riva, A.; Rossetti, S.; Zini, L.; Casagrande, G.; et al. Differentiated spring behavior under changing hydrological conditions in an alpine karst aquifer. *J. Hydrol.* **2018**, *556*, 572–584, doi:10.1016/j.jhydrol.2017.11.040.
5. Şener, A.; Yolcubal, I.; Ercan, S. Determination of recharge, storage and flow characteristics of a karst aquifer using multi-method approaches (Kocaeli, Turkey. *Hydrogeol. J.* **2020**, *28*, 2141–2157.
6. White, W.B. *Geomorphology and Hydrology of karst terrains*; Oxford University: Oxford, UK, 1988.
7. Bakalowicz, M. Karst groundwater: A challenge for new resources. *Hydrogeol. J.* **2005**, *13*, 148–160, doi:10.1007/s10040-004-0402-9.
8. Mook, W.G. Environmental isotopes in the hydrological cycle; *Tech. Doc. Hydrol.* **2000**, *1*, 1–291.
9. Dansgaard, W. Stable isotopes in precipitation. *Tellus* **1964**, *16*, 436–468, doi:10.3402/tellusa.v16i4.8993.

10. Jasechko, S. Global Isotope Hydrogeology—Review. *Rev. Geophys.* **2019**, *57*, 835–965, doi:10.1029/2018RG000627.
11. Longinelli, A.; Selmo, E. Isotope geochemistry and the water cycle: A short review with special emphasis on Italy. *Cart. Geol. D'Italia XC* **2010**, *90*, 153–164.
12. Giustini, F.; Brilli, M.; Patera, A. Mapping oxygen stable isotopes of precipitation in Italy. *J. Hydrol. Reg. Stud.* **2016**, *8*, 162–181, doi:10.1016/j.ejrh.2016.04.001.
13. Calligaris, C.; Mezga, K.; Slejko, F.F.; Urbanc, J.; Zini, L. Groundwater characterization by means of conservative (δ18O and δ2H) and non-conservative (87Sr/86Sr) isotopic values: The classical karst region aquifer case (Italy–Slovenia). *Geosci.* **2018**, *8*, 1–25, doi:10.3390/geosciences8090321.
14. Phillips, F.M. The use of isotopes and environmental tracers in subsurface hydrology. *Rev. Geophys.* **1995**, *33*, 1029–1033, doi:10.1029/95RG00247.
15. Hartmann, A.; Goldscheider, N.; Wagener, T.; Lange, J.; Weiler, M. Karst water resources in a changing world: Review of hydrological modeling approaches. *Rev. Geophys.* **2014**, *52*, 218–242, doi:10.1002/2013RG000443.
16. González-Trinidad, J.; Pacheco-Guerrero, A.; Júnez-Ferreira, H.; Bautista-Capetillo, C.; Hernández-Antonio, A. Identifying groundwater recharge sites through environmental stable isotopes in an alluvial aquifer. *Water (Switzerland)* **2017**, *9*, 1–12, doi:10.3390/w9080569.
17. Sappa, G.; Vitale, S.; Ferranti, F. Identifying karst aquifer recharge areas using environmental isotopes: A case study in central Italy. *Geosci.* **2018**, *8*, doi:10.3390/geosciences8090351.
18. Wachniew, P. Environmental tracers as a tool in groundwater vulnerability assessment. *Acque Sotter. - Ital. J. Groundw.* **2015**, 19–25, doi:10.7343/as-108-15-0135.
19. Arellano, L.N.; Good, S.P.; Sánchez-murillo, R.; Jarvis, W.T.; Noone, D.C.; Finkenbiner, C.E. Bayesian estimates of the mean recharge elevations of water sources in the Central America region using stable water isotopes. *J. Hydrol. Reg. Stud.* **2020**, *32*, 100739, doi:10.1016/j.ejrh.2020.100739.
20. Vespasiano, G.; Apollaro, C.; Rosa, R. De; Muto, F.; Larosa, S.; Fiebig, J.; Mulch, A.; Marini, L. Applied Geochemistry The Small Spring Method (SSM) for the de fi nition of stable isotope e elevation relationships in Northern Calabria (Southern Italy). *Appl. Geochemistry* **2015**, *63*, 333–346, doi:10.1016/j.apgeochem.2015.10.001.
21. Iacurto, S.; Grelle, G.; Filippi, F.M.D.; Sappa, G. Karst spring recharge areas and discharge relationship by oxygen-18 and deuterium isotopes analyses: A case study in southern latium region, Italy. *Appl. Sci.* **2020**, *10*, doi:10.3390/app10051882.
22. Thornthwaite, C.W. An Approach toward a Rational Classification of Climate. *Geogr. Rev.* **1948**, *38*, 55–94, doi:10.2307/210739.
23. Civita, M.; De Maio, M.; Vigna, B. Una metodologia GIS per la valutazione della ricarica attiva degli acquiferi. In Proceedings of the Convegno Nazionale sulla Protezione e Gestione delle Acque Sotterranee ; Parma, Italy, 13–15 October 1999.
24. Tulipano, L.; Sappa, G.; Pietrellli, G. Groundwater Budget of Maiella (Italy). In Proceedings of the Balancing the groundwater Budget; Darwin, Australia, 12–17 May 2002; pp. 1–7.
25. Canora, F.; Sdao, F. Hydrogeological characterization and groundwater vulnerability to pollution assessment of the high basento river valley carbonate hydrostructure (Basilicata, Southern Italy). *Ital. J. Eng. Geol. Environ.* **2020**, *20*, 25–44, doi:10.4408/IJEGE.2020-01.O-03.
26. Sappa, G.; De Filippi, F.M.; Iacurto, S.; Grelle, G. Evaluation of minimum karst spring discharge using a simple rainfall-input model: The case study of Capodacqua di Spigno Spring (Central Italy). *Water (Switzerland)* **2019**, *11*, doi:10.3390/w11040807.
27. Ialongo, N. *Studio Idrogeologico Sorgente Mazzoccolo*; Relazione Idrogeologica: Formia, Italy, 1983.
28. Baldi, A.M.; Marzocchi, A.; Ricci, A.; Mencarini, S.; Vecellio, L.; Graziosi, A.; Di Mauro, G. La torbidità alle captazioni idropotabili dei monti Aurunci. In Proceedings of the Aquifer Vulnerability and Risk, Parma, Italy, 21–23 September 2005.
29. Bergomi, C.; Catenacci, V.; Cestari, G.; Manfredini, M.; Manganelli, V. Note illustrative della carta geologica d'Italia, alla scala 1:100.000—Foglio 171 Gaeta e Vulcano di Roccamonfina; Ercolano, Poligrafica & cartevalori: Naples, Italy, 1969.
30. Craig, H. Isotopic variations in meteoric waters. *Science (80-.).* **1961**, *133*, 1702–1703, doi:10.1126/science.133.3465.1702.
31. NEMS (National Environmental Monitoring Standards) *Open Channel Flow measurement*; Version 1.1; 2013. Availale online: https://www.lawa.org.nz/media/16578/nems-open-channel-flow-measurement-2013-06.pdf (accessed on 14 July 2021).
32. Sappa, G.; Ferranti, F.; Iacurto, S.; De Filippi, F.M. Effects of climate change on groundwater feeding the Mazzoccolo and Capodacqua di Spigno Springs (Central Italy): First quantitative assestments. In Proceedings of the International Multidisciplinary Scientific GeoConference Surveying Geology and Mining Ecology Management, SGEM, Albena, Bulgaria, 30 June–9 July 2018; Volume 18.
33. White, W.B. Karst hydrology: Recent developments and open questions. *Eng. Geol.* **2002**, *65*, 85–105, doi:10.1016/S0013-7952(01)00116-8.
34. Yang, Q.; Mu, H.; Guo, J.; Bao, X.; Martín, J.D. Temperature and rainfall amount effects on hydrogen and oxygen stable isotope in precipitation. *Quat. Int.* **2019**, *519*, 25–31, doi:10.1016/j.quaint.2019.01.027.
35. Bard, E.; Delaygue, G.; Rostek, F.; Antonioli, F.; Silenzi, S.; Schrag, D.P. Hydrological conditions over the western Mediterranean basin during the deposition of the cold Sapropel 6 (ca. 175 Kyr BP). *Earth Planet. Sci. Lett.* **2002**, *202*, 481–494, doi:10.1016/S0012-821X(02)00788-4.
36. Higgins, P.; MacFadden, B.J. "Amount Effect" recorded in oxygen isotopes of Late Glacial horse (Equus) and bison (Bison) teeth from the Sonoran and Chihuahuan deserts, southwestern United States. *Palaeogeogr. Palaeoclimatol. Palaeoecol.* **2004**, *206*, 337–353, doi:10.1016/j.palaeo.2004.01.011.

37. Li, Z.; Li, Z.; Zhao, W.; Wang, Y. Probability modeling of precipitation extremes over two river basins in northwest of China. *Adv. Meteorol.* **2015**, *2015*, doi:10.1155/2015/374127.
38. Bono, R.; Gonfiantini, R.; Alessio, M.; Fiori, C.; D'Amelio, C. Stable isotopes (δ18O, δ2H) and tritium in precipitation: Results and comparison with groundwater perched aquifers in central Italy. In Isotopic Composition ofPrecipitation in the MediterraneanBasin in Relationto Air Circulation Patternsand Climate, Final Report a Coordinated Research Project, 2000–2004; Isotope Hydrology Section, International Atomic Energy Agency: Vienna, Austria, 2005.
39. Dumas, D. The impact of forests on the evolution of water resources in the mid-altitude Alps from the middle of the 19th. *Rev. géographie Alp.* **2012**, doi:10.4000/rga.1632.
40. Palcsu, L.; Gessert, A.; Túri, M.; Kovács, A.; Futó, I.; Orsovszki, J.; Puskás-Preszner, A.; Temovski, M.; Koltai, G. Long-term time series of environmental tracers reveal recharge and discharge conditions in shallow karst aquifers in Hungary and Slovakia. *J. Hydrol. Reg. Stud.* **2021**, *36*, 100858, doi:10.1016/j.ejrh.2021.100858.
41. Jódar, J.; Herms, I.; Lambán, L.J.; Martos-Rosillo, S.; Herrera-Lameli, C.; Urrutia, J.; Soler, A.; Custodio, E. Isotopic content in high mountain karst aquifers as a proxy for climate change impact in Mediterranean zones: The Port del Comte karst aquifer (SE Pyrenees, Catalonia, Spain). *Sci. Total Environ.* **2021**, *790*, 148036, doi:10.1016/j.scitotenv.2021.148036.
42. Tulipano, L.; Fidelibus, D.M.; Panagopoulos, A. *Groundwater Management of Coastal Karstic Aquifers: Final Report*; EU Publications Office: Luxemburg, 2005.